

# Effect of liposomal confinement on photochemical properties of photosensitizers with varying hydrophilicity

Isabelle Noiseux  
Ozzy Mermut  
Jean-Pierre Bouchard  
Jean-François Cormier  
Patrice Desroches  
Michel Fortin  
Pascal Gallant  
Sébastien Leclair  
Marcia L. Vernon

INO (National Optics Institute)  
Department of Biophotonics  
2740 Einstein Street  
Québec G1P 4S4, Canada

Kevin R. Diamond  
Michael S. Patterson

McMaster University  
and  
Juravinski Cancer Center  
Department of Medical Physics and Applied Radiation  
Sciences  
Hamilton, 699 Concession Street  
Ontario L8V 5C2, Canada

**Abstract.** Preferential tumor localization and the aggregation state of photosensitizers (PSs) can depend on the hydrophilic/hydrophobic nature of the molecule and affect their phototoxicity. In this study, three PSs of different hydrophilicity are introduced in liposomes to understand the structure-photochemistry relationship of PSs in this cellular model system. Absorbance and fluorescence spectra of amphiphilic aluminum (III) phthalocyanine disulfonate chloride adjacent isomer (Al-2), hydrophilic aluminum (III) phthalocyanine chloride tetrasulfonic acid (Al-4), and lipophilic 2-(1-hexyloxyethyl)-2-devinyl pyropheophorbide (HPPH) are compared in a liposomal confined state with free PS in bulk solution. For fluorescence measurements, a broad range of concentrations of both bulk and liposomal confined PSs are examined to track the transition from monomers to dimers or higher order aggregates. Epifluorescence microscopy, absorbance, and fluorescence measurements all confirm different localization of the PSs in liposomes, depending on their hydrophilicity. In turn, the localization affects the aggregation of molecules inside the liposome cell model. Data obtained with such cellular models could be useful in optimizing the photochemical properties of photosensitizing dyes based on their structure-dependent interactions with cellular media and subcellular organelles. © 2008 Society of Photo-Optical Instrumentation Engineers. [DOI: 10.1117/1.2950309]

**Keywords:** Photosensitizers; fluorescence; photodynamic therapy; liposome cell model; hydrophilicity.

Paper 07380SSR received Sep. 14, 2007; revised manuscript received Jan. 29, 2008; accepted for publication Mar. 3, 2008; published online Jul. 15, 2008. This paper is a revision of a paper presented at the SPIE conference on Therapeutic Laser Applications and Laser-Tissue Interactions III, June 2007, Munich, Germany. The paper presented there appears (unrefereed) in SPIE Proceedings Vol. 6632.

## 1 Introduction

Photodynamic action is a light-activated process that photochemically induces the production of cytotoxic singlet oxygen. The process is mediated by the transfer of energy from an optically excited photosensitizer (PS) molecule to molecular oxygen (activation via type-II pathway).<sup>1</sup> This singlet oxygen causes critical damage to the surrounding tissues via apoptosis or necrosis of the cancer cells. Photodynamic therapy is an established modality, where the PSs used for treatment have largely evolved with knowledge of the mechanisms of action.<sup>2</sup> Criteria for development of second-generation PSs include: absorption in the red region of the spectra to enable deeper light penetration, good quantum yield for intersystem crossing and energy transfer to oxygen, monomer conformation (as aggregation of PS may decrease the phototoxicity and affect the localization in cells), high uptake and selectivity for cancer cells, and no dark toxicity.<sup>3-6</sup> Photosensitizers can be administered either topically or systemically. Topical application is highly selective to the lesion of interest, but the depth

of treatment is limited to the absorption of the PS into the surface and the penetration of the excitation light. In systemic applications, the PS goes to all lesions, even those that have not been previously identified, and the treatment volume is limited to those regions accessible to a light source (e.g., interstitial optical fiber).

In principle, the efficiency of tumor photosensitization is dependent on the molecular-scale chemical properties of the PS and the photochemical consequences of intracellular localization.<sup>7-9</sup> For example, the structure, charge, and hydrophobicity of a PS govern its intra- and intermolecular interactions (e.g., aggregation and affinity to biological cellular constituents). This in turn dictates pharmacological properties such as: efficiency and specificity of cellular uptake, subcellular localization, and phototoxicity.<sup>8,10</sup> The efficacy of photodynamic therapy is related to the interplay of direct cell killing, vascular damage, inflammation, and immune host response.<sup>10-12</sup>

It has been reported that amphiphilic PSs are more photodynamically active and achieve better tumor localization than either symmetrically hydrophobic or hydrophilic molecules.<sup>3,10</sup> Disulfonated phthalocyanines may be synthe-

Address all correspondence to: Ozzy Mermut, Department of Biophotonics, INO, 2740, Einstein St., Québec, QC, Canada G1P 4S4. Tel: 418-657-7006; Fax: 418-657-7009; e-mail: ozzy.mermut@ino.ca.

sized in two configurations, either on opposite sides of the ring or at adjacent pyrrolic positions. For example, in the sulfonated phthalocyanine series, the most efficient PS *in vitro* is 2-adjacent-sulfonated positions, followed by 1-, 3-, 2-opposite and 4-derivatives.<sup>7</sup> While purely hydrophilic drugs have less tendency to aggregate, they do not exhibit optimal phototoxicity<sup>3,8</sup> compared to amphiphilic PSs, which typically display enhanced photodynamic potency both *in vitro* and *in vivo*. It has been hypothesized that the improved phototoxic efficacy in amphiphilic PSs is related to preferential localization at hydrophobic-hydrophilic interfaces in membranes.<sup>7,10</sup> The amphiphilicity of a PS also controls the degree of aggregation in aqueous biological media, leading to distinctive photophysical and photochemical properties. For example, Al-2 dimers display specific absorption bands, representative of either stacked (700 nm) or staggered (640 nm) conformers.<sup>13–15</sup>

Since much of the damage to cells results from high uptake of PS in the various cellular membranes (e.g., mitochondria), drugs that bind preferentially to membranes, in an unaggregated form, are desirable.<sup>5,10</sup> The damage done to plasma and organelle membranes include electric depolarization, increased permeability, membrane rupture, and cell lysis.<sup>16–18</sup> However, many of the second-generation PSs are highly hydrophobic and display poor tumor selectivity. Highly lipophilic PSs have a tendency to aggregate in aqueous media, especially when no organic solvent is used, which impairs their photophysical properties.<sup>19</sup> Previous studies have established that an increase in the monomeric equilibrium population of a PS is associated with increased photodynamic action.<sup>4</sup> Rosenfeld et al.<sup>20</sup> found that modifying the exocyclic ring of pyropheophorbides including 2-(1-hexyloxyethyl)-2-devinyl pyropheophorbide (HPPH) caused a decrease in the photosensitizing efficiency due to a decrease in solubility and increased aggregation, associated with lower tumor uptake and decreased singlet oxygen production. By confining a PS in biologically compatible delivery systems intrinsically amphiphilic in nature, such as liposomes, it is possible to: increase solubilization of highly hydrophobic PSs, preferentially drive PS molecules toward monomeric species suitable for photodynamic therapy (PDT), formulate them in a preparation suitable for intravenous (i.v.) administration, increase circulation time and uptake by tumor cells, and increase tumor selectivity.<sup>6</sup> In this scheme, the use of organic solvents for *in-vivo* application is also avoided.

Liposomes are vesicles composed of an aqueous core enclosed by a bilayer of phospholipids forming the membrane. Having important applications in nanomedicine, liposome technology was developed to improve the pharmacokinetics and the bioavailability of therapeutics.<sup>21,22</sup> The incorporation of PS molecules in liposomes has previously been shown to enhance their phototoxicity significantly.<sup>23–25</sup> This simple vesicular construct not only makes liposomes useful as drug carriers, but one can envision them as simplified models for cell membranes or subcellular structures. Moreover, the physical, optical, and chemical properties of liposomes can be tuned to mimic specific properties of targeted tumor cells and their biomembrane constituents (e.g., by varying its size from micro—to nanometers), degree of lamellarity/interfaces, and membrane chemical composition. Liposomes have already been used as models mimicking *in vivo* situations to study the

influence of physicochemical, photobiological, and biomedical factors that directly impact the uptake of PSs, their mechanism of action, and the subsequent photoreactions.<sup>26</sup> Several studies have been conducted to establish the impact of substituting different side-chains on PS molecules on aggregation or fluorescent properties inside liposome bilayers,<sup>25,27–31</sup> to clarify liposomal interactions without inclusion of PS in the bilayer,<sup>5,32</sup> and to establish the consequences of PS incorporation in liposomes by comparing with free PS in different solvents.<sup>24,33</sup>

In this study, we introduce three different PSs into liposomes, used as a cell model. To understand the photophysical properties of PSs in this cell model, optically homogeneous preparations are used to control the scattering and absorbing properties observed in inhomogeneous systems like tissues. We restricted ourselves to PSs having strong absorption bands in the near-IR-visible range, known as the “therapeutic spectral window.” In this spectral window, attenuation by hemoglobin is minimized and scattering is reduced, which permits more treatment light to reach the tumor, activating more drug.<sup>3,4</sup> The three PSs are agents that have suitable photochemical and photophysical properties for PDT (i.e., high triplet-state quantum yield, low dark toxicity, high uptake and retention *in vivo*, and effective tumor photosensitization), namely, aluminum phthalocyanine Al-2 and Al-4 (containing two and four ionizable sulfonate moieties) and Photochlor® (HPPH). Photosensitizers of varying hydrophobicity and structure were selected according to their localization properties, a result of the balance between the hydrophobicity and hydrophilicity of the PS and lipid bilayer.<sup>34</sup> The motivation for selecting HPPH (a new phase I/II drug) comes from recent studies, which indicate that HPPH has unique pharmacokinetic properties owing to its lipophilicity.<sup>35</sup>

To understand the structure-photochemistry relationship, we investigated differences in the spectroscopic properties of in-solution and liposome-confined PSs (L-PSs). The experiments were conducted in identical biocompatible solvents. Fluorescence properties were measured over a concentration range covering two orders of magnitude, to probe the conformational transition of the PSs from monomer to dimer and higher order aggregates associated with high concentrations. Having understood the effect of L-PS confinement on the photochemical properties, we conducted further studies to establish the impact of confinement on the fluorescence lifetime behavior in liposome models (reported in part companion work, see Ref. 36).

## 2 Materials and Methods

### 2.1 Materials

The photosensitizers aluminum (III) phthalocyanine chloride tetrasulfonic acid (Al-4) and aluminum (III) phthalocyanine disulfonate chloride adjacent isomer (Al-2) were purchased from Frontier Scientific, Incorporated, UT, USA. The photosensitizer 2-(1-hexyloxyethyl)-2-devinyl pyropheophorbide (HPPH) was kindly provided by Roswell Park Cancer Institute. Liposomes were prepared using 1,2-dioleoyl-*sn*-glycero-3-phosphocholine (DOPC) and cholesterol (CHOL, Northern Lipids Incorporated, B.C., Canada). Solvents used in bulk solution and liposome studies were either phosphate-buffered saline (PBS, pH 7.4) or 20:80 fetal bovine serum (FBS)/PBS

**Table 1** Average liposome sizes and concentrations of L-PSs used after separation.

L-PS	Average vesicle size (nm)	Initial concentration (liposome/mL)	Concentration of L-PSs solutions (liposome/mL)					
			L-A	L-B	L-C	L-D	L-E	L-F
L-AI-2	138±47	$6.6 \times 10^7$	$2.7 \times 10^7$	$9.1 \times 10^6$	$3.0 \times 10^6$	$1.0 \times 10^6$	$3.4 \times 10^5$	$1.1 \times 10^5$
L-AI-4	134±45	$8.8 \times 10^7$	$2.7 \times 10^7$	$9.1 \times 10^6$	$3.0 \times 10^6$	$1.0 \times 10^6$	$3.4 \times 10^5$	$1.1 \times 10^5$
L-HPPH	132±43	$7.4 \times 10^7$	$2.7 \times 10^7$	$9.1 \times 10^6$	$3.0 \times 10^6$	$1.0 \times 10^6$	$3.4 \times 10^5$	$1.1 \times 10^5$
L-blank	132±43	$2.7 \times 10^8$	$2.7 \times 10^7$	—	—	—	—	—

(Sigma) dissolved in Milli-Q ultrapure water (UV-treated 18.2 M $\Omega$ ·cm resistivity). Solutions were filtered through a Nalgene 0.45- $\mu$ M filter to remove scattering contaminants.

## 2.2 Liposome Preparation with Photosensitizers and Spectral Characterization

Liposomes were prepared by dissolving 50 mg of DOPC and 8.6 mg (35%mol) of CHOL in chloroform. The chloroform was subsequently roto-evaporated until a uniform thin lipid film was formed. This lipid cake was hydrated by drop-wise additions of PS (5.0 mL) at 40 °C, and swirling, over 30 min. The photosensitizer concentrations used were 50- $\mu$ M AI-4 in PBS, 25- $\mu$ M AI-2 in PBS (presonicated to aid solubility), and 100- $\mu$ M HPPH in PBS/PBS. The hydrated phospholipids were agitated and resuspended by rotating on a roto-evaporator (180 rpm) without applying vacuum for 15 min at 65 °C. The resulting liposomes were subjected to 10 freeze-thaw cycles to induce stability (at -80 °C and 60 °C, respectively). The liposomes were extruded 11 times through a 100-nm pore-size polycarbonate membrane to ensure a narrow size distribution. Vesicle size and distribution were determined for both liposomes incorporating PSs (L-PS) and blank liposomes containing only PBS (L-blank). Particle sizing was based on dynamic light scattering measurements (DLS) acquired at varying angles between 90 to 150 deg (BI9000 apparatus from Brookhaven Instruments at 532 nm using BI200SM goniometer and B2FBK/RFI PMT). The vesicle sizes from Gaussian/Nicomp distribution analysis (intensity weighted) were tightly grouped around a single mean value (135 nm). Free PSs were removed from the solution containing encapsulated PSs using Sephadex G-25 prepacked size exclusion columns (NAP 5, GE Healthcare). Images of the L-PSs were acquired with an epifluorescence inverted microscope (Eclipse TE2000-U, Nikon) equipped with a charge-coupled device (CCD) camera (QICAM fast 1394, QImaging) and 100 $\times$  objective. The absorption spectra of the bulk PS solutions used for liposomal preparation and the confined L-PS solutions corresponding to the highest concentration (sample A) were recorded with a spectrophotometer (Cary500, Varian). Fluorescence measurements of a range of concentrations of bulk PS solution and L-PS were performed with a spectrofluorometer (Cary Eclipse, Varian) using 661-nm excitation. The emission was collected with a band-

pass filter (680 to 710 nm) identical to that used for fluorescence lifetime studies (Ref. 36), allowing direct comparison between spectral and temporal studies.

## 2.3 Flow Cytometry

The liposome vesicle concentration of each sample was determined by flow cytometry using the fluorescence channel, since a portion of the liposome's distribution size was too small to be adequately detected by forward scattering. The fluorescence channel was then used directly as a gate. The liposomes were analyzed using an EPICS Elite ESP (Beckman Coulter) device equipped with a 633-nm He-Ne laser at 10 mW. The fluorescence emission was separated from the excitation light by using a 650-nm dichroic mirror and a bandpass filter centered at 670 nm. Fluorescent calibration beads were used to align the laser to minimize the coefficient of variation induced by the device itself.

The liposome concentration (quantity of liposomes per milliliter) were subsequently adjusted to the same value for all L-PS samples. The blank liposome concentration was determined by bilayer labeling with Nile Red (Sigma).<sup>37</sup> No separation of unbound Nile Red was performed, as this dye selectively fluoresces when attached to lipids.<sup>38,39</sup> The concentration of L-blank (unlabeled) liposomes were subsequently matched to the L-PS concentrations.

## 3 Results

### 3.1 Physical Characterization of Liposomes

PSs AI-2, AI-4, and HPPH were incorporated in liposomes separately, and L-blank was prepared for background comparison. After the extrusion step, the average liposome size was determined, summarized in Table 1. It was observed that the mean vesicle diameter was similar for all preparations, 135 ± 45 nm. Once the PSs were incorporated into the liposomes, the unencapsulated PSs were removed from the media by size exclusion separation (not performed for L-blank). The variable retention of liposomes in the size exclusion column is a dynamic and reversible known process.<sup>40</sup> Therefore, the exact amount of liposomes lost due to separation was quantified by flow cytometry, and found to depend on the specific PS incorporated. The resulting liposome concentrations were  $6.6 \times 10^7$ ,  $8.8 \times 10^7$ , and  $7.4 \times 10^7$  liposomes mL<sup>-1</sup> for L-AI-2, L-AI-4, and L-HPPH, respectively. These results in-

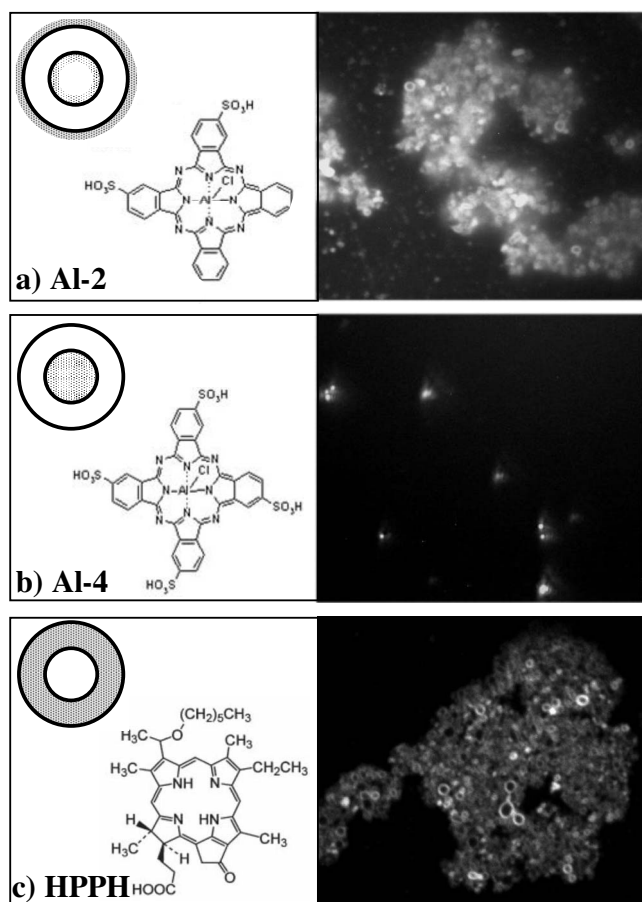


**Fig. 1** Epifluorescence microscope images of confined PSs (in poly-disperse liposomes) with their chemical structure and suggested schematic of the PS liposomal localization of (a) L-Al-2, (b) L-Al-4, and (c) L-HPPH.

dicating that the liposome retention in the column was not the same for every L-PS, and may be related to the spatial localization of PS within the liposome particles traveling through the Sephadex material. Using the flow cytometry data, linear dilutions were performed to achieve a liposome concentration series ranging from  $2.7 \times 10^7$  liposomes  $\text{mL}^{-1}$  (concentration A) to  $1.1 \times 10^5$  liposomes  $\text{mL}^{-1}$  (concentration F).

### 3.2 Microscopic Characterization of Confined Photosensitizers

Examination of the three selected PSs chemical structures, particularly the acid-base properties of the substituents, revealed very different hydrophilic-hydrophobic properties (Fig. 1). Consequently, it is expected that there will be structure-dependent, preferential localization of PS within a liposome.<sup>13</sup> Figure 1 presents images of the confined PSs in liposomes obtained by epifluorescence microscopy. To aid visualization, these pictures were derived from highly concentrated solutions containing large, polydisperse liposomes. Accompanying Fig. 1 are schematic representations of the PSs spatial confinement in liposomes suggested by the fluorescence micrographs.

Figure 1(a) shows fluorescence emitted both from the liposome membrane and the core of L-Al-2. In contrast, the fluo-

rescence observed in L-HPPH [Fig. 1(c)] arises solely from the bilayer membrane. Previous studies of AlPcSn in cationic reversed micelles suggest that amphiphilic molecules, such as Al-2, tend to localize at the interface of the lipid/core construct.<sup>13</sup> Hence, the localization of Al-2 is believed to occur at both the internal and external interface of the phospholipid bilayer, explaining the diffuse pattern of the fluorescence observed in Fig. 1(a). The highly hydrophilic nature of Al-4, arising from the tetrasulfonate substituents, is believed to drive this PS primarily to the aqueous core of the liposome. Indeed, Fig. 1(b) confirms the hydrophilicity argument, and Al-4 fluorescence is mainly observed inside the central cavity of the vesicle. As HPPH is highly lipophilic,<sup>41</sup> fluorescence is only detected from hydrophobic domains of the liposome, defined strictly by the phospholipid boundary [Fig. 1(c)].

### 3.3 Liposomal Confinement of Amphiphilic Photosensitizers

Figure 2 presents the absorption and fluorescence emission spectra for different concentrations of free Al-2 in bulk solution, as well as confined in liposomes. The characteristics of the absorbance spectra of monomeric phthalocyanines in bulk solution are well documented. A strong Soret peak around 350 nm, a weak maximum around 600 nm, and a narrow, very strong Q-band absorption peak in the far-red region of the visible spectra around 670 nm have been reported previously.<sup>4,13-15,42</sup> However, phthalocyanines in water tend to form dimers and higher order aggregates due to the propensity of the large hydrophobic skeleton to avoid contact with an aqueous medium.<sup>13</sup> Dimer formation can be observed spectroscopically, as the Q-band exhibits a decrease in the extinction coefficient and a blueshift to  $\sim 640$  nm for the staggered dimers, or a redshift toward  $\sim 700$  nm for the stacked dimers.<sup>13</sup> Extended dimerization causes a large decrease of the extinction coefficient of the Q-band with broadening of the band over a spectral range from 550 to 800 nm. The Soret absorption peak is also broadened and shifted toward a shorter wavelength.<sup>14,15</sup> Less spectral information is available concerning the higher order aggregates of phthalocyanines in solution.

The absorption spectrum [Fig. 2(a)] of Al-2 shows a Soret peak at 354 nm, a weak maximum at 605 nm, a strong Q-band at 672 nm, and the weaker dimer band at 642 nm.<sup>4,13</sup> Al-2 is considered less hydrophilic (i.e., less soluble in water) than Al-4, because it has two fewer sulfonic acid groups, as shown in Fig. 1(a). As such, a smaller concentration of Al-2 ( $25 \mu\text{M}$ ) was prepared with the aid of presonication, while complete solubility was achieved at  $50 \mu\text{M}$  Al-4. Al-2 is thus considered an amphiphilic PS exhibiting both hydrophobic and hydrophilic properties.<sup>8</sup> The liposomal confinement of Al-2 produced a slight redshift in the absorption Soret and Q-bands, as shown in Table 2.

The excitation of Al-2 at 661 nm yielded a fluorescence emission peak at 684 nm. Note that the expected peaks above 710 nm with different PSs were not detected due to the use of a bandpass filter (680 to 710 nm). The intensity of the fluorescent peak at 684 nm increased with Al-2 concentration in bulk solution up to  $10 \mu\text{M}$ , after which the intensity decreased concomitant with a redshift in the maximum peak emission to 687 and 691 nm for 25 and  $50 \mu\text{M}$ , respectively

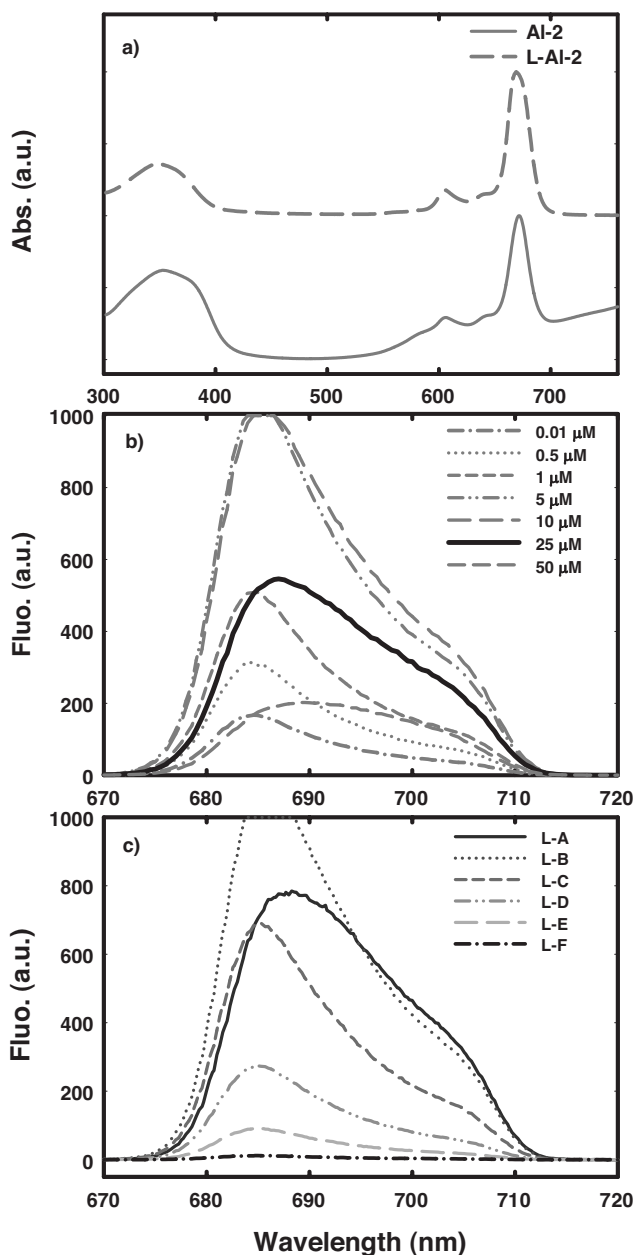


**Fig. 2** (a) Normalized absorbance spectra of bulk solution Al-2 ( $25 \mu\text{M}$ , solid line) versus confined L-Al-2 (dashed line). (b) Fluorescence emission spectra of bulk Al-2, and (c) liposome L-Al-2 as a function of PS concentration and liposome concentration (defined in Table 1), respectively.

[Fig. 2(b)]. The same trend was observed with increasing concentrations of liposomes containing Al-2 [Fig. 2(c)]. At the smallest concentration of liposomes (F), there was negligible fluorescence. The increase of L-Al-2 concentration caused an increase of peak fluorescence intensity until concentration B was reached, after which fluorescence saturation occurred as observed by decrease in the fluorescence signal concomitant with redshifting of concentration A. At concentration A, the fluorescence intensity decrease was similar to what was observed in bulk solution, with a small associated redshift (685 to 688 nm). It should be noted here that for all experiments, each liposome contained approximately the same amount of PS; it was the increase of liposome concentration that caused the increase in the effective concentration of Al-2 in the sample. All PS concentrations introduced to the lipid cake were kept high (and approximately identical at  $\sim 50 \mu\text{M}$ , within solubility limit), to allow for comparison at maximum drug incorporation for each L-PS. However, the absolute encapsulation efficiency of the PS into liposomes was unknown. The confinement of Al-2 provided a unique lipophilic/aqueous interface facilitating greater solubility of Al-2 molecules.

### 3.4 Liposomal Confinement of Hydrophilic Photosensitizers

The absorption spectrum of tetrasulfonated phthalocyanine, Al-4, also presents a Soret (350 nm) and Q-bands (674 and 606 nm), as shown in Fig. 3(a). Containing four sulfonic acid substituents, Al-4 is the most hydrophilic of the three PSs. Unlike Al-2, Al-4 did not exhibit an aggregate absorption band at  $\sim 640$  nm. It was expected that an increase of the number of sulfonate moieties in the phthalocyanine should produce more intensive repulsion between rings, and therefore, minimize aggregation.<sup>13</sup> As evidenced by similar curves obtained for AL-4 and L-Al-4 [Fig. 3(a)], the absorption properties of Al-4 were not affected by the confinement in liposomes.

Excitation of free solution Al-4 in the low concentration range (1 to  $10 \mu\text{M}$ ) resulted in a strong fluorescence emission peak centered at 685 nm. In the higher concentration regime, a pronounced redshift from 691 to 696 nm was observed when incrementing the concentration from 25 to  $50 \mu\text{M}$ , accompanied by a significant decrease in the relative fluorescence intensity of 50%. While both free solutions of Al-2 and Al-4 were redshifted at higher concentrations, the magnitude of this effect was larger in the case of

**Table 2** Summary of maximum peaks in absorbance and fluorescence spectra of bulk and liposomal-containing PS.

Ps	Absorption max peaks (nm)		Fluorescence max peaks (nm)	
	Bulk	Liposome	Bulk	Liposome
Al-2	353, 605, 642, 672	349, 605, 642, 669	689	688
Al-4	350, 606, 674	350, 605, 674	694	685
HPPH	398, 667	421, 665	692	684

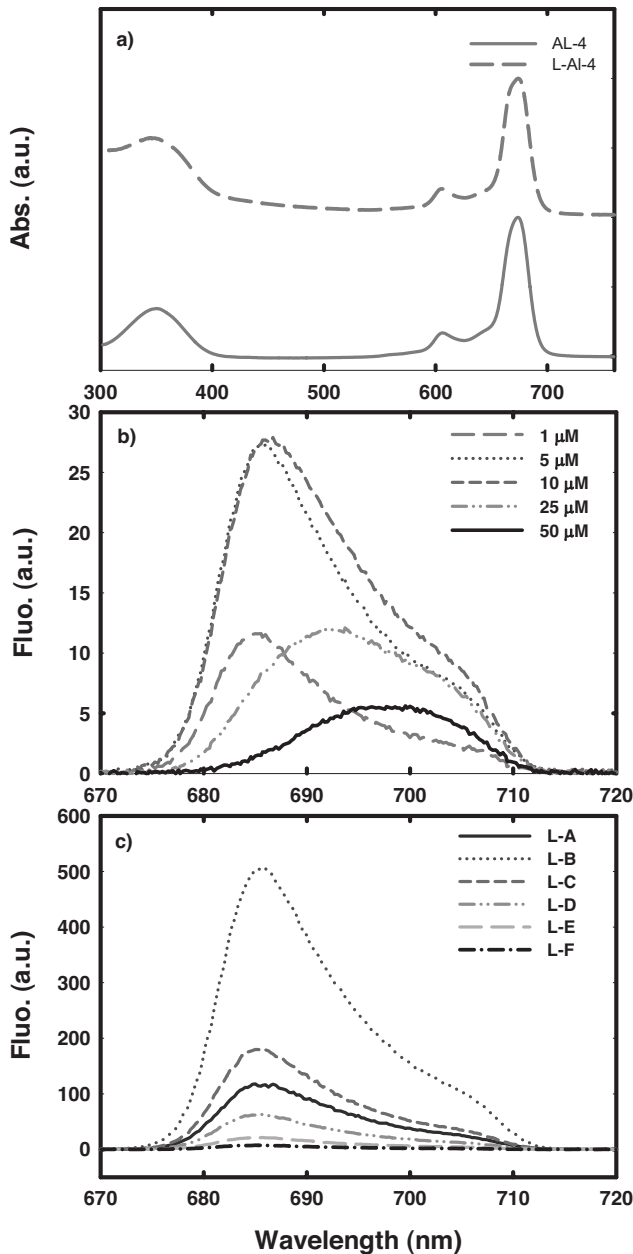


**Fig. 3** (a) Normalized absorbance spectra of bulk solution Al-4 (50  $\mu\text{M}$ , solid line) versus confined L-Al-4 (dashed line). (b) Fluorescence emission spectra of bulk Al-4, and (c) liposome L-Al-4 as a function of PS concentration and liposome concentration, respectively.

hydrophilic Al-4. In the case of liposome-confined Al-4, the primary fluorescence emission peak at 685 nm was not affected by changes in liposome concentration, as seen across the range shown in Fig. 3(c). The fluorescence intensity increased with concentration up to concentration B, but decreased at the maximum L-Al-4 concentration A, which was associated with a 1-nm redshift.

### 3.5 Liposomal Confinement of Lipophilic Photosensitizer

The third PS, HPPH, is a new drug that is currently undergoing clinical testing. Information on this PS is limited, particu-

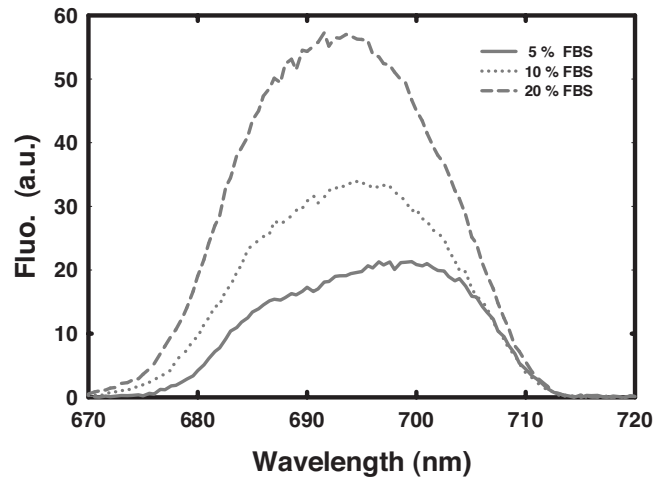


**Fig. 4** Fluorescence emission spectra of bulk solution HPPH (100  $\mu\text{M}$ ) as a function of relative FBS content in PBS solvent.

larly in the context of liposomal confinement, but there is some spectral information available reporting two main absorption peaks (408 and 665 nm) and fluorescence emission located approximately at 675 nm with shoulder above 700 nm.<sup>43,44</sup> The two main absorption peaks for the bulk solution were observed at 398 and 667 nm, with the presence of small peaks located approximately at 508, 540, and 607 nm. Those small peaks, with the one located at 667 nm, are called Q-bands and were also present on the absorbance spectra in many other studies.<sup>43,45–48</sup> Even though those peaks are reported in the literature, little information is available on the link between the chemical structure of HPPH and the presence of those peaks, or the impact of aggregate states on the molar extinction and wavelength dependence of these Q-bands.

HPPH has been described as lipophilic, as its carboxylic groups are ionized at physiological pH. This PS has been found to be localized in intracellular membranes, namely in endoplasmic reticulum, Golgi apparatus, lysosomes, and mitochondria.<sup>47,49</sup> The liposomal confinement of this lipophilic PS induced a change in the shape of the Soret absorption peak, which becomes narrower and better defined, shifting the maximum from 398 to 421 nm and decreasing the intensity of the far-red band. The inclusion of HPPH in the phospholipids/CHOL membrane also modifies the distribution of the Q-bands. The hydrophobic tail of the phospholipid provides a microenvironment that favors solubilization of the PS in the membrane of the liposome and thus reduces the aggregation.

In a bulk solution of PBS, HPPH has a very low fluorescence quantum yield. To achieve higher fluorescence intensities, different solvents were used to solubilize this PS (Fig. 4). Addition of FBS produced an increase in the fluorescence emission of HPPH. Specifically, changing the FBS fraction from 5 to 20% in the PBS solvent produced a significant increase, greater than two fold, in the fluorescence intensity at identical concentrations. A significant gain in intensity was obtained when HPPH was solubilized in 20:80 FBS/PBS, and this optimized solvent mix was used in all subsequent experiments. The absorbance contribution of FBS/PBS was negli-

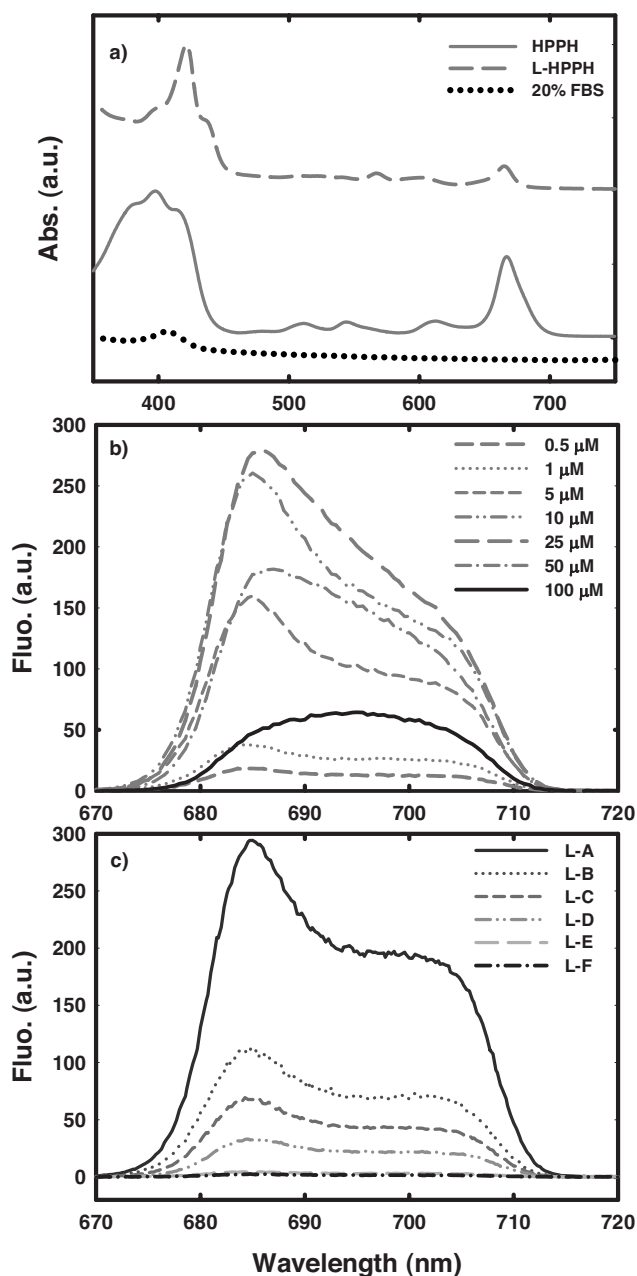


**Fig. 5** (a) Normalized absorbance spectra of bulk solution HPPH ( $100 \mu\text{M}$ , solid line) versus confined L-HPPH (dashed line) and background FBS solvent (dotted line). Fluorescence emission spectra of (b) bulk Al-4, and (c) liposome L-Al-4 as a function of PS concentration and liposome concentration, respectively.

gible, as shown in Fig. 5(a), and no fluorescence was emitted from this solvent when excited at 661 nm. The intensity of the HPPH fluorescence increased with increasing concentrations up to  $25 \mu\text{M}$  [Fig. 5(b)], with a prominent emission peak at 685 nm and a shoulder around 702 nm. At concentrations above  $25 \mu\text{M}$ , a redshifting occurs in which the relative contribution of the shoulder increases. At the highest concentration of  $100 \mu\text{M}$ , one broad peak is identified concomitant with redshift to 695 nm. When the PS was confined in liposomes, the fluorescence emission signal of L-HPPH was found to increase with increasing concentration of liposomes

from F to A. The shoulder observed in the bulk solution was also present in L-HPPH. In contrast to the free solution of HPPH, and unlike the other PS molecules investigated, no decrease in the intensity or redshifting was observed through the entire concentration series of L-HPPH.

## 4 Discussion

Structure, charge, and hydrophobicity determine the cellular uptake, subcellular localization, and phototoxicity of PSs. As a result, Al-2, Al-4, and HPPH were selected for spectral analysis based on the variability in these properties. From the acid/base properties and number of peripheral substituents (a single carboxylic acid for HPPH and di- and tetra-sulfonate for Al-2 and Al-4, respectively, shown in Fig. 1), the relative hydrophobicity scale of the PSs studied here was HPPH > Al-2 > Al-4. The goal of the study was to establish the relationship between PS molecular properties and the expected cellular localization relevant to photodynamic treatment, using simplified cell models. While liposomes are often used as drug carriers, we employed them as cellular phantoms to mimic the drug uptake and localization. It was suggested that the liposomal localization of these PSs is based on their respective hydrophilic/hydrophobic properties, residual charge, and structure. To validate this hypothesis, PS fluorescence was compared for free and liposome-confined PSs over a wide concentration range spanning >2 orders of magnitude. Although the absolute uptake of the liposomal system was not determined, we supplied a high concentration of PS solution for liposome incorporation to maximize the encapsulation efficiency.

### 4.1 Photosensitizer Behavior in Bulk Solution

We compared the absorbance spectra of bulk PS solutions (identical to those used in the L-PS formulation) to that of the highest L-PS concentration prepared (concentration set A) [Figs. 2(a), 3(a), and 5(a)]. Comparison of the absorbance spectra provides insight on the aggregation behavior of PSs in liposomes and bulk solution. From Fig. 3(a), it is clear that even at high concentrations ( $50 \mu\text{M}$ ), bulk Al-4 presents no aggregation products that absorb in the visible range, also observed by Juzenas et al.<sup>42</sup> Liposomal encapsulation to L-Al-4 did not change the absorbance features. However, the absorbance spectrum of Al-2 (at the maximum concentration of  $25 \mu\text{M}$ ) exhibited some aggregation characteristics. Specifically, the Soret peak and Q-band were redshifted from 349 to 353 nm and from 669 to 672 nm, respectively, and the overall absorbance was higher in the red region of the spectrum for the bulk Al-2 compared to the L-Al-2.

In the case of the hydrophobic porphyrin molecule HPPH, two main absorption peaks at 408 and 665 nm, with three small peaks located approximately at 508, 540, and 607 nm, were observed, as reported previously.<sup>43,44</sup> In bulk solution, the photophysical properties of porphyrins with negatively charged peripheral substituents change due to the aggregation process.<sup>50</sup> Dimers and higher aggregates modify the absorption and fluorescence spectra: dimers cause shifting toward shorter wavelength and an increase in the width of the Soret band at full width at half-maximum (FWHM), with redshifting of the Q-band,<sup>30,45</sup> and higher order aggregates typically shift the Soret peak to 360 nm and cause a large redshift of

the principle Q-band.<sup>46</sup> The spectra of nonaggregated porphyrins typically show a linear decrease in the intensity of the Q-bands with increasing wavelength, a behavior known as *etio*-type spectrum.<sup>25</sup>

Liposome formulations with highly concentrated solutions (*i.e.*, where PSs are in dimer conformation) displace the equilibria toward monomerization and lipid localization.<sup>27,51</sup> Redshifts in the Soret and Q-bands were also observed with liposomal confinement but were typically small. Kuciauskas et al.<sup>33</sup> reported that changing the solvent of the porphyrin [5,10,15,20 - tetrakis - (4-hydroxyphenyl) -21,23H-porphyrin] from acetone to a liposome without cholesterol caused a redshift of the Soret and Q-bands of 1 to 4 nm. Encapsulation of the PS in the ordered lipid bilayer can also change the symmetry of the PS molecule and simplify its absorption spectrum into a two-band system. Changes in symmetry due to membrane incorporation, and its consequences on absorption, are analogous in mechanism to the effect of peripheral substituents on the inductive polarization of the chromophore.<sup>45</sup> Hence, the structure of a porphyrin, the local microenvironment, including the solvent used and the dye concentration, will determine the contribution from monomers, dimers, and higher order aggregates to the net spectroscopic properties. It has been reported that even in liposomes, where the equilibrium favors monomerization, some contributions from aggregate species are always present.<sup>50</sup>

Based on the observation of the Soret peak position and broad FWHM of the HPPH absorbance spectrum [Fig. 5(a)], we can state that aggregates are present in the highly concentrated bulk solution. Also, the Q-bands do not appear as an *etio*-type spectrum. In fact, the three low absorbance Q-bands (508, 540, and 607 nm) had approximately the same intensity, while the red band (665 nm) had a relatively higher intensity, similar to previous results obtained with 2.5  $\mu\text{M}$  of three different chlorine derivatives in tetrahydrofuran (THF).<sup>24</sup> Following liposomal confinement, the Soret band was redshifted and the FWHM was narrower, suggestive of monomerization of the HPPH. The Q-bands were simplified to a two band system, a consequence of PS incorporation into a highly ordered bilayer of phospholipids. The absorption spectra obtained in liposomes were similar to those obtained by Kuciauskas et al.<sup>33</sup> for other hydrophobic porphyrins in acetone solvent and in liposomes. In a manner analogous to the effect of acetone, the polarity of the solvent influenced the effective solubilization of HPPH in a phospholipid environment. It has been suggested that the hydrophobic core structure of porphyrins can be effectively embedded deep in the aliphatic chain of the phospholipids, while its carboxylic substituent(s) may either interact with the polar head of the phospholipid or with the cholesterol situated between the phospholipids.<sup>27,33,51</sup>

From the absorbance spectra, it was observed that at high concentrations, HPPH and Al-2 tend to form dimers or higher order aggregates, as opposed to hydrophilic Al-4, which is highly soluble and not aggregated, even at high concentrations. The fluorescence spectra of the three PSs were acquired over a broad concentration range for both the free solution and the corresponding liposome-confined analogs. For all the bulk solutions, results show that the fluorescence intensity increased with concentration until a maximum was reached, after which the intensity decreased concomitant with a redshift in the emission peak maximum. In the case of ptha-

locyanines, there is a debate in the literature about the decrease of fluorescence intensity at high PS concentration and the redshift associated with this phenomenon. The decrease in emission intensity is often attributed to the formation of the commonly encountered cofacial phthalocyanine dimers that are reported to be nonfluorescent and photodynamically inactive.<sup>14,45,52</sup> In their studies, redshifting of fluorescence peaks has been identified and associated with dimer emission.<sup>53,54</sup> However, among the nonfluorescent dimers, some fluorescent species have been observed but emission is restricted to particular species.<sup>55,56</sup> At room temperature and pH=7.2, the decreases in intensity observed for Al-2 and HPPH may in part be explained by the presence of dimers or higher order aggregates that are present at high concentrations and that do not fluoresce. This is supported by the absorbance spectra obtained for Al-2 and HPPH at high concentrations [25 and 100  $\mu\text{M}$ , respectively, Figs. 2(a) and 5(a)]. However, the contribution of aggregate quenching to the fluorescence signal may not entirely account for the total decrease in the fluorescence intensity observed and the concomitant redshift, especially at high concentrations. For example, the contribution of dimers or higher order aggregates was not evident from the absorbance spectrum of Al-4 at 50  $\mu\text{M}$  (Fig. 3), although a reduction in fluorescence intensity and redshift were observed with increasing PS concentration. Hence, the decrease in fluorescence intensity with increasing concentration may in part be associated with self-absorption, a common optical phenomenon known to occur particularly at higher fluorophore concentrations.<sup>15,57,58</sup>

Self-absorption occurs when a portion of the fluorescence emission is reabsorbed by neighboring fluorophores due to the overlap of the absorption and emission bands of the fluorophore. This in itself has the effect of shifting the apparent peak emission of the observed fluorescence. Moreover, a fraction of these reabsorbed photons are re-emitted, thus increasing further the redshift in the emission peak wavelength. This phenomenon is typically observed at high fluorophore concentrations and/or when the "effective" light path length is large, as the result of scattering, for example.<sup>59</sup> The total fraction of photons that will be reabsorbed and re-emitted depends on several geometric and chemical factors, including the concentration. Increasing the fluorophore concentration improves the probability that photons are reabsorbed and re-emitted, with the redshift becoming more apparent, observed for all free PSs in aqueous solution over the concentration range studied [Figs. 2(b), 3(b), and 5(b)]. The concentration at which the intensity starts to decrease and where the redshift becomes apparent is PS dependent and related to their respective Stokes shift and fluorescence quantum yield. The observed redshift, although similar for Al-2 and HPPH ( $\sim 8$  nm), was found to be higher for Al-4 ( $\sim 12$  nm). Some Al-2 and HPPH molecules are present as dimers or higher order aggregates when the concentration of PS in solution is high. This presence of nonfluorescent conformations decreases the effective concentration of fluorescent species that can re-emit redshifted photons. This may explain the smaller degree of redshift with Al-2 and HPPH and explains the large redshift observed for Al-4, which is negligibly aggregated.

## 4.2 Photosensitizer Fluorescence in Liposomes

The fluorescence study of liposome-confined L-AI-2 showed a similar trend of redshifting at the highest liposome concentrations; increasing the liposome concentration from F to A had the same results on the measured fluorescence as increasing the bulk concentration. A redshift and decrease in fluorescence intensity were observed at the highest concentrations B and A. While the uptake efficiency of AI-2 in liposomes was not known, the spatial localization of the PS, shown in the epifluorescence image, and the amphiphilic properties of AI-2 suggested that it resides at the membrane interface (on the external and/or internal bilayer surface). Interfacial alignment of amphiphilic *cis* AI-2 molecules on similar membrane surfaces has been reported previously.<sup>13,60</sup> The trends observed in bulk AI-2 and L-AI-2 as a function of concentration were similar. This is because the liposomal localization of the amphiphilic AI-2 molecules did not result in encapsulation as in the case of L-AI-4, which has its local concentration of fluorescing species maintained within the core of the liposome. The localization of AI-2 on the surface of the liposome membrane means that the PS can interact with other surface-bound PS molecules. Consequently, as the liposome concentration is increased, we observe the corresponding red-shift that mirrors the fluorescence behavior observed in free solution AI-2.

The liposomal membrane is constituted of DOPC, an unsaturated phospholipid, and a significant quantity of cholesterol (35 mol %) to mimic cellular membrane chemistry. The lipid molecules are highly mobile in membranes. For example, the unsaturated fatty acids of membrane lipids rotate easily. Cholesterol is a key constituent in the cell membrane having a critical role on membrane organization, function, and sorting.<sup>61</sup> It is also known to improve the tendency for stable vesicles to form by facilitating hydrophobic interactions in the bilayer.<sup>62</sup> Lipids are known to undergo lateral diffusion, an effect that generally decreases with increasing cholesterol content. DOPC phospholipids incorporating cholesterol are relatively disordered, imparting more motion and fluidity into the membranes via transmembrane “flip-flop” movement.<sup>63,64</sup> Given that cholesterol has pronounced effects on the structural properties of membranes, PS molecules localized within or near the surface of the bilayer display high sensitivity to membrane dynamics. As such, it is not surprising that interfacial AI-2 molecules, located on the external interface of the liposomal membranes, are highly mobile, allowing intra- and interliposomal aggregation, consequently producing the reabsorption and re-emission effects observed here. Although the concentration of liposome is relatively low, interliposomal aggregation is seen with L-AI-2 [Fig. 1(a)] which facilitates interaction of interfacial AI-2 molecules. Conversely, no interliposome aggregation is present in the case of L-AI-4, as evidenced by Fig. 1(b).

For L-AI-4, an increase in fluorescence intensity with liposome concentration was not accompanied by a redshift. Attributed to its hydrophilicity, the bulk absorbance spectrum of AI-4 was without aggregation bands, and the epifluorescence image showed the PS to be confined primarily to the core volume of the liposome. Previous reports suggested that due to its tetrasulfonate substitution with strong acids, AI-4 is highly soluble and stable in water, and does not form aggregates as observed in the visible spectral range.<sup>42</sup> Hence, con-

finement into the aqueous core of the liposomes was not expected to cause a spectral shift in the fluorescence emission pattern. The liposomes prepared in this experiment had a mean diameter of 130 nm, which resulted in a liposome volume of  $9.2 \times 10^{-21} \text{ m}^3$ . Considering that the highest liposome concentration used was  $2.7 \times 10^7 \text{ mL}^{-1}$ , we estimate that the PS-containing liposome volume fraction in solution was  $2.5 \times 10^{-7}$ . Assuming that the liposome solution was a homogeneous colloidal suspension, we can estimate that the mean distance between liposomes in solution was approximately 33  $\mu\text{m}$ . Since AI-4 molecules were encapsulated inside the liposome core, the molecules were restricted to interact intraliposome only. The small liposome volumic fraction of PS and the larger mean inter-liposome distance implies that there was a low chance that emitted photons from L-AI-4 in one liposome would be reabsorbed by L-AI-4 molecules residing in another liposome. Reabsorption and re-emission depends not only on the concentration of the fluorophores in solution, but also on the average optical pathlength of the fluorescence inside the solution itself. Based on the calculated average optical pathlength, reabsorption effects for core-confined L-AI-4 were believed to be negligible.<sup>58,59</sup> Therefore, the confinement of hydrophilic AI-4 PS inside the core volume of the liposome created a homogenous and protected microenvironment over the large range of liposome concentrations studied here. Hence, reabsorption and re-emission phenomena of PS molecules via interliposome interactions were not significant, as compared to those in bulk aqueous solution. Consequently, increasing the liposome concentration over 2 orders of magnitude also produced fluorescence redshifting like that observed in bulk solution with increasing concentration.

The increase of the L-HPPH concentration resulted in increased fluorescence intensity for all concentrations, with no redshifting or aggregation observed. Although the uptake efficiency of liposomes was unknown for HPPH, the lipophilic nature of the PS suggests that the molecule was driven to the inside of the liposomal membrane, where it is stabilized by the nonpolar domain of the phospholipid. The fact that no spectral modifications were observed at the highest concentration of L-HPPH can be explained by both optical and chemical arguments. Despite the relatively high concentrations of HPPH used for liposomes, no detection of re-emission due to reabsorption was detected. Also, the average optical path length of PS embedded in the liposome membrane was small enough to assess that the reabsorption of fluorescence was insignificant.<sup>58,59</sup> Chemical considerations of hydrophobic interaction initiated from membrane incorporation of HPPH suggest that the phospholipid bilayer of the liposome provided an environment that favored monomeric HPPH. Furthermore, the low liposomal volumic fraction indicated that the mean interliposomal distance was large compared to their size, minimizing interliposome HPPH interactions. The liposomal confinement of HPPH created a lipophilic microenvironment where the number of HPPH in close proximity was low, protected by the membrane from any interaction with other PS molecules despite aggregation of liposomes, as observed in Fig. 1(c).

## 4.3 Implication of Photosensitizer Localization

The localization of PS is important for efficient PDT. One reason is that singlet oxygen diffuses rapidly out of mem-

branes, and thus efficient reactions with its target are necessary for phototoxicity generated in lipid membranes.<sup>32</sup> The microenvironment of PSs in cells also affects aggregation which has a deleterious effect on photodynamic activity. Hence, PS drugs need to be introduced into the bloodstream in a form that is either monomeric, or easily dissociated by the plasma. For IV administration, hydrophobic PSs require formulations that minimize aggregation *in vivo*, like liposomal vehicles that favor the monomeric form of the PS. Amphiphilic PSs have been reported as being excellent candidates for liposomal formulation.<sup>59</sup> Studies are currently under way in our laboratory to corroborate the results observed in our model system with PS localization effects in cells.

## 5 Conclusion

Two of the three PSs tested (HPPH and Al-2) in this study display some degree of dimerization or higher order aggregates when present in high concentrations in solution. Those nonfluorescent species were responsible, in part, for the decrease in the intensity of the fluorescence emission. However, at high PS concentrations, the quenching of fluorescence and the concomitant redshift are explained by the reabsorption and re-emission of fluorescence. The localization of PSs in liposomes is dependent on the balance between hydrophilicity/hydrophobicity of the molecules and their affinity with the bilayer. Hydrophilic Al-4 is mainly localized inside the aqueous core of the liposome, while the lipophilic HPPH is mainly distributed in the phospholipid bilayer; these localizations tend to prevent interliposome interactions of the PSs. However, the amphiphilic Al-2, localized at the interface of the membrane, is a highly dynamic system where interliposome interactions between PSs are possible.

## Acknowledgments

This work has been financially supported in part by Canadian Institutes of Health Research (CIHR) and CIHR (IG) RMS-79069. We are grateful to Barbara Henderson and the Photodynamic Therapy Center of Roswell Park Cancer Institute for providing HPPH. We thank McGill University for assistance with the dynamic light scattering measurements.

## References

1. L. I. Grossweiner, "Photodynamic therapy: Science and technology," Chap. 10 in *The Science of Phototherapy: An Introduction*, L. R. Jones, J. B. Grossweiner, and B. H. G. Rogers, Eds., pp. 243–275, Springer, Norwell, MA (2005).
2. S. B. Brown, E. A. Brown, and I. Walker, "The present and the future role of photodynamic therapy in cancer treatment," *Lancet Onc.* **5**(8), 497–508 (2004).
3. R. Bonnett, "Photosensitizers of the porphyrin and phthalocyanines series for photodynamic therapy," *Chem. Soc. Rev.* **24**(1), 19–33 (1995).
4. C. M. Allen, W. M. Sharman, and J. E. Van Lier, "Current status of phthalocyanines in the photodynamic therapy of cancer," *J. Porphyr. Phthalocyanines* **5**(2), 161–169 (2001).
5. A. Lavi, H. Weitman, R. T. Holmes, K. M. Smith, and B. Ehrenberg, "The depth of porphyrin in a membrane and the membrane's physical properties affect the photosensitizing efficiency," *Biophys. J.* **82**(4), 2101–2110 (2002).
6. B. Chen, B. W. Pogue, and T. Hasan, "Liposomal delivery of photosensitizing agents," *Expert Opin. Biol. Ther.* **2**(3), 477–487 (2005).
7. P. Margaron, M. J. Grégoire, V. Scasnár, H. Ali, and J. E. Van Lier, "Structure-photodynamic activity relationships of a series of 4-substituted zinc phthalocyanines," *Photochem. Photobiol.* **63**(2), 217–223 (1996).
8. C. M. Allen, R. Langlois, W. M. Sharman, C. La Madeleine, and J. E. Van Lier, "Photodynamic properties of amphiphilic derivatives of aluminum tetrasulfophthalocyanine," *Photochem. Photobiol.* **76**(2), 208–216 (2002).
9. Y. You, S. L. Gibson, R. Hilf, S. R. Davies, A. R. Oseroff, I. Roy, T. Y. Ohulchanskyy, E. J. Bergey, and M. R. Detty, "Water soluble, core-modified porphyrins. 3. Synthesis, photophysical properties, and *in vitro* studies of photosensitization, uptake, and localization with carboxylic acid-substituted derivatives," *J. Med. Chem.* **46**(17), 3734–3747 (2003).
10. I. J. MacDonald and T. J. Dougherty, "Basic principles of photodynamic therapy," *J. Porphyr. Phthalocyanines* **5**(2), 105–129 (2001).
11. T. J. Dougherty, C. J. Gomer, B. W. Henderson, G. Jori, D. Kessel, M. Koberlik, J. Moan, and Q. Peng, "Photodynamic therapy," *J. Natl. Cancer Inst.* **90**(12), 889–905 (1998).
12. K. Kalka, H. Merk, and H. Mukhtar, "Photodynamic therapy in dermatology," *J. Am. Acad. Dermatol.* **42**(3), 389–413 (2000).
13. S. Dharni, J. J. Cosa, S. M. Bishop, and D. Phillips, "Photophysical characterization of sulfonated aluminum phthalocyanines in a cationic reversed micellar system," *Langmuir* **12**(2), 293–300 (1996).
14. R. B. Ostler, A. D. Scully, A. G. Taylor, I. R. Gould, T. A. Smith, A. Waite, and D. Phillis, "The effect of pH on the photophysics and photochemistry of di-sulfonated aluminum phthalocyanine," *Photochem. Photobiol.* **71**(4), 397–404 (2000).
15. Z. Petrášek and D. Phillips, "A time-resolved study of concentration quenching of disulfonated aluminum phthalocyanine fluorescence," *Photochem. Photobiol. Sci.* **2**(3), 236–244 (2003).
16. K. G. Specht and M. A. J. Rodgers, "Plasma membrane depolarization and calcium influx during cell injury by photodynamic action," *Biochim. Biophys. Acta* **1070**(1), 60–68 (1991).
17. M. Paardekooper, P. J. A. Van den Broek, A. W. De Bruijn, J. G. R. Elferink, T. M. A. R. Dubbelman, and J. Van Steveninck, "Photodynamic treatment of yeast cells with dye Toluidine blue: All-or-none loss of plasma membrane barrier properties," *Biochim. Biophys. Acta* **1108**(1), 86–90 (1992).
18. D. Kessel and Y. Luo, "Intracellular sites of photodamage as a factor in apoptotic cell death," *Photochem. Photobiol.* **5**(2), 181–184 (2001).
19. X. Peng, E. Sternberg, and D. Dolphin, "Separation of porphyrin-based photosensitizer isomers by laser-induced fluorescence capillary electrophoresis," *Electrophoresis* **26**(20), 2861–2868 (2005).
20. A. Rosenfeld, J. Morgan, L. N. Goswami, T. Ohulchanskyy, X. Zheng, P. N. Prasad, A. Oseroff, and R. K. Pandey, "Photosensitizers derived from 13<sup>2</sup>-oxo-methyl pyropheophorbide-a: enhanced effect of indium(III) as a central metal in *in vitro* and *in vivo* photosensitizing efficacy," *Photochem. Photobiol.* **82**(3), 626–634 (2006).
21. S. Sengupta and R. Sasisekharan, "Exploiting nanotechnology to target cancer," *Br. J. Cancer* **96**(9), 1315–1319 (2007).
22. V. Wagner, A. Dullaart, A.-K. Bock, and A. Zweck, "The emerging nanomedicine landscape," *Nat. Biotechnol.* **24**(10), 1211–1217 (2006).
23. A. S. L. Derycke, A. Kamuhabwa, A. Gijssens, T. Roskams, D. De Vos, A. Kasran, J. Huwyler, L. Missiaen, and P. A. A. de Witte, "Transferrin-conjugated liposome targeting of photosensitizer AlPcS<sub>4</sub> to rat bladder carcinoma cells," *J. Natl. Cancer Inst.* **96**(21), 1620–1630 (2004).
24. F. Postigo, M. L. Sagristá, M. A. de Madariaga, S. Nonell, and M. Mora, "Photosensitization of skin fibroblasts and HeLa cells by three chlorin derivatives: role of chemical structure and delivery vehicle," *Biochim. Biophys. Acta* **1758**(5), 583–596 (2006).
25. G. Kramer-Marek, C. Serpa, A. Szurko, M. Widel, A. Sochanik, M. Sniatura, P. Kus, R. M. D. Nunes, L. G. Arnaut, and A. Ratuszna, "Spectroscopic properties and photodynamic effects of new lipophilic porphyrin derivatives: efficacy, localization and cell death pathways," *J. Photochem. Photobiol., B* **84**(1), 1–14 (2006).
26. M. Hoebeke and X. Damoiseau, "Determination of the singlet oxygen quantum yield of bacteriochlorin a: a comparative study in phosphate buffer and aqueous dispersion of dimristoyl-L-phosphatidylcholine liposomes," *Photochem. Photobiol. Sci.* **1**(4), 283–287 (2002).
27. D. Brault, "Physical chemistry of porphyrins and their interactions with membranes: the importance of pH," *J. Photochem. Photobiol., B* **6**(1–2), 79–86 (1990).

28. F. Ricchelli, S. Gobbo, G. Moreno, C. Salet, L. Brancaleon, and A. Mazzini, "Photophysical properties of porphyrin planar aggregates in liposomes," *Eur. J. Biochem.* **253**(3), 760–765 (1998).
29. N. G. Angeli, M. G. Lagorio, E. A. San Román, and L. E. Dixelio, "Meso-substituted cationic porphyrins of biological interest. Photo-physical and photochemical properties in solution and bound to liposomes," *Photochem. Photobiol.* **72**(1), 49–56 (2000).
30. K. Das, A. Dube, and P. K. Gupta, "A spectroscopic study of photobleaching of chlorine p6 in different environments," *Dyes Pigm.* **64**(3), 201–205 (2005).
31. S. Ben-Dror, I. Bronshtein, A. Wiehe, B. Röder, M. O. Senge, and B. Ehrenberg, "On the correlation between hydrophobicity, liposome binding and cellular uptake of porphyrin sensitizers," *Photochem. Photobiol.* **82**(3), 695–701 (2006).
32. I. Bronshtein, M. Afri, H. Weitman, A. A. Frimer, K. M. Smith, and B. Ehrenberg, "Porphyrin Depth in lipid bilayers as determined by iodide and parallax fluorescence quenching methods and its effect on photosensitizing efficiency," *Biophys. J.* **87**(2), 1155–1164 (2004).
33. D. Kuciauskas, C. J. Wohl, M. Pouy, A. Nasai, and V. Gulbinas, "Nonlinear optical spectroscopic studies of energy transfer in phospholipid bilayer liposomes embedded with porphyrin sensitizers," *J. Phys. Chem. B* **108**(39), 15376–15384 (2004).
34. K. Lang, J. Mosinger, and D. M. Wagnerová, "Photophysical properties of porphyrinoid sensitizers non-covalently bound to host molecules; models for photodynamic therapy," *Coord. Chem. Rev.* **248**(3–4), 321–350 (2004).
35. B. W. Henderson, D. A. Bellnier, W. R. Greco, A. Sharman, R. K. Pandey, L. A. Vaughan, K. R. Weishaupt, and T. J. Dougherty, "An *in vivo* quantitative structure-activity relationship for a congeneric series of pyropheophorbide derivatives as photosensitizers for photodynamic therapy," *Cancer Res.* **57**, 4000–4008 (1997).
36. O. Mermut, I. Noiseux, J. P. Bouchard, J. F. Cormier, P. Desroches, M. Fortin, P. Gallant, S. Leclair, M. L. Vernon, K. R. Diamond, and M. S. Patterson, "Effect of liposomal confinement on photothermal and photo-oximetric fluorescence lifetimes of photosensitizers with varying hydrophilicity," *J. Biomed. Opt.* **13**, 041314 (2008).
37. P. Greenspan and S. D. Fowler, "Spectrofluorometric studies of the lipid probe, Nile red," *J. Lipid Res.* **26**(7), 781–789 (1985).
38. G. Hungerford, A. L. F. Baptista, P. J. G. Coutinho, E. M. S. Castanheira, and M. E. C. D. R. Oliveira, "Interaction of DODAB with neutral phospholipids and cholesterol studied using fluorescence anisotropy," *J. Photochem. Photobiol., A* **181**(1), 99–105 (2006).
39. E. Feitosa, F. R. Alves, A. Niemic, M. E. C. D. R. Oliveira, E. M. S. Castanheira, and A. L. F. Baptista, "Cationic Liposomes in mixed didodecyltrimethylammonium bromide and dioctadecyltrimethylammonium bromide aqueous dispersions studied by differential scanning calorimetry, Nile red fluorescence, and turbidity," *Langmuir* **22**(8), 3579–3585 (2006).
40. T. Ruyschaert, A. Marque, J. L. Duteyrat, S. Lesieur, M. Winterhalter, and D. Fourmier, "Liposome retention in size exclusion chromatography," *BMC Biotech.* **5**(11), 1472–6750-5–11 (2005).
41. D. A. Bellnier, W. R. Greco, G. M. Loewen, H. Nava, A. R. Oseroff, R. K. Pandey, T. Tsuchida, and T. J. Dougherty, "Population pharmacokinetics of the photodynamic therapy agent 2-[1-hexyloxyethyl]-2-devinyl pyropheophorbide-a in cancer patients," *Cancer Res.* **63**(8), 1806–1813 (2003).
42. P. Juzenas, A. Juzeniene, R. Rotomskis, and J. Moan, "Spectroscopic evidence of monomeric aluminum phthalocyanine tetrasulphonate in aqueous solutions," *J. Photochem. Photobiol., B* **75**(1–2), 107–110 (2004).
43. J. D. Wilson, W. J. Cottrell, and T. H. Foster, "Index-of-refractive-dependent subcellular light scattering observed with organelle-specific dyes," *J. Biomed. Opt.* **12**(1), 014010-1–014010-10 (2007).
44. D. A. Bellnier, W. R. Greco, H. Nava, G. M. Loewen, A. R. Oseroff, and T. J. Dougherty, "Mild skin photosensitivity in cancer patients following injection of photochlor (2-[1-hexyloxyethyl]-2-devinyl pyropheophorbide-a; HPPH) for photodynamic therapy," *Cancer Chemother. Pharmacol.* **57**(1), 40–45 (2006).
45. E. Reddi and G. Jori, "Steady-state and time-resolved spectroscopic studies of photodynamic sensitizers: Porphyrins and phthalocyanines," *Rev. Chem. Intermed.* **10**(3), 241–268 (1988).
46. G. J. Smith, K. P. Ghiggino, L. E. Bennett, and T. L. Nero, "The Q-band absorption spectra of hematoporphyrin monomer and aggregate in aqueous solution," *Photochem. Photobiol.* **49**(1), 49–52 (1989).
47. X. Sun and W. N. Leung, "Photodynamic therapy with pyropheophorbide-a methyl ester in human lung carcinoma cancer cell: efficacy, localization and apoptosis," *Photochem. Photobiol.* **75**(6), 644–651 (2002).
48. D. M. Chen, X. Liu, T. J. He, and F. C. Liu, "Density functional theory investigation of porphyrin diacid: electronic absorption spectrum and conformational inversion," *Chem. Phys.* **289**(2–3), 397–407 (2003).
49. I. J. MacDonald, J. Morgan, D. A. Bellnier, G. M. Paszkiewicz, J. E. Whitaker, D. J. Litchfield, and T. J. Dougherty, "Subcellular localization patterns and their relationship to photodynamic activity of pyropheophorbide-a derivatives," *Photochem. Photobiol.* **70**(5), 789–797 (1999).
50. F. Ricchelli, "Photophysical properties of porphyrins in biological membranes," *J. Photochem. Photobiol., B* **29**(2–3), 109–118 (1995).
51. R. Margalit and S. Cohen, "Studies of hematoporphyrin and hematoporphyrin derivative equilibria in heterogeneous systems," *Biochim. Biophys. Acta* **736**(2), 163–170 (1983).
52. A. Beeby, S. FitzGerald, and C. F. Stanley, "Protonation of tetrasulfonated zinc phthalocyanine in aqueous acetonitrile solution," *Photochem. Photobiol.* **74**(4), 566–569 (2001).
53. M. Yoon, Y. Cheon, and D. Kim, "Absorption and fluorescence spectroscopic studies on dimerization of chloroaluminum (III) phthalocyanine tetrasulfonate in aqueous alcoholic solutions," *Photochem. Photobiol.* **58**(1), 31–36 (1993).
54. Y. Kaneko, T. Arai, K. Tokumaru, D. Matsunaga, and H. Sakuragi, "Observation of a novel fluorescent dimer of zinc tetrasulphonatophthalocyanine," *Chem. Lett.* **25**(5), 345–346 (1996).
55. N. M. Speirs, W. J. Ebenezer, and A. C. Jones, "Observation of a fluorescent dimer of a sulfonated phthalocyanine," *Photochem. Photobiol.* **76**(3), 247–251 (2002).
56. S. FitzGerald, C. Farren, C. F. Stanley, A. Beeby, and M. R. Bryce, "Fluorescent phthalocyanine dimers—a steady state and flash photolysis study," *Photochem. Photobiol. Sci.* **1**(8), 581–587 (2002).
57. J. R. Lackowitz, "Time-domain lifetime measurements, frequency-domain lifetime measurements, and advanced topics in fluorescence quenching," Chaps. 4, 5, and 9 in *Principles of Fluorescence Spectroscopy*, pp. 95–162, 267–278, Kluwer Academic/Plenum, New York (1999).
58. P. P. Pompa, G. Ciccarella, J. Spadavecchia, R. Cingolani, G. Vasapollo, and R. Rinaldi, "Spectroscopic investigation of inner filter effects by phthalocyanine solutions," *J. Photochem. Photobiol., A* **163**(1–2), 113–120 (2004).
59. J. F. Cormier, M. Fortin, J. Fréchette, I. Noiseux, M. L. Vernon, and W. Long, "The effects of self-absorption and detection geometry on fluorescence intensity and decay lifetime," *Proc. SPIE* **5702**, 123–134 (2005).
60. J. A. Lacey and D. Phillips, "Fluorescence lifetime measurements of disulfonated aluminum phthalocyanine in the presence of microbial cells," *Photochem. Photobiol. Sci.* **1**(6), 378–383 (2002).
61. S. Mukherjee, H. Raghuraman, and A. Chattopadhyay, "Membrane localization and dynamics of Nile red: Effect of cholesterol," *Biochim. Biophys. Acta* **1768**(1), 59–66 (2007).
62. W. Wang, X. Qu, A. I. Gray, L. Tetley, and I. F. Uchebgu, "Self assembly of cetyl linear polyethylenimine to give micelles, vesicles and nanoparticles is controlled by the hydrophobicity of the polymer," *Macromolecules* **37**(24), 9114–9122 (2004).
63. P. L. Yeagle, "Cholesterol and the cell membrane," *Biochim. Biophys. Acta* **822**(3–4), 267–287 (1985).
64. A. Filippov, G. Orädd, and G. Lindblom, "The effect of cholesterol on the lateral diffusion of phospholipids in oriented bilayers," *Bio-phys. J.* **84**(5), 3079–3086 (2003).